A Navier-Stokes-Korteweg Model for Dynamic Wetting based on the PeTS Equation of State

Felix Diewald[1,*], **Michaela Heier**[2], **Martin Lautenschläger**[2], **Martin Horsch**[3], **Charlotte Kuhn**[4], **Kai Langenbach**[2], **Hans Hasse**[2], and **Ralf Müller**[1]

[1] Institute of Applied Mechanics, TU Kaiserslautern, 67653 Kaiserslautern, Germany

[2] Laboratory of Engineering Thermodynamics, TU Kaiserslautern, 67653 Kaiserslautern, Germany

[3] Scientific Computing Department, Daresbury Laboratory, Warrington WA4 4AD, UK

[4] Computational Mechanics, TU Kaiserslautern, 67653 Kaiserslautern, Germany

Dynamic wetting of component surfaces can be investigated by finite element phase field simulations. Often these models use a double-well potential or the van der Waals equation to define the local part of the free energy density at a point of the computational domain. In order to give the present model a stronger physical background the molecular dynamics based perturbed Lennard-Jones truncated and shifted (PeTS) equation of state is used instead. This results in phase field liquid-vapor interfaces that agree with the physical density gradient between the two phases. In order to investigate dynamic scenarios, the phase field description is coupled to the compressible Navier-Stokes equations. This coupling requires a constitutive equation that complies with the surface tension of the liquid-vapor interface resulting from the PeTS equation of state and is comparable to the so-called Korteweg tensor.

1 Phase Field Model

The Phase Field (PF) model used in this work couples the Navier-Stokes equations with the static PF model described in [1]. The coupling is done via the capillary stress tensor described by Korteweg in 1901, see e.g. [2]. Therefore, the model can be classified as a Navier-Stokes-Korteweg model. A central component of Navier-Stokes-Korteweg models is the equation of state that formulates the free energy density of the bulk phases as well as the transition zone between them. Instead of applying the commonly used van der Waals equation of state, the present model utilizes the PeTS equation of state [3] which provides an accurate energy density formulation for the Lennard-Jones truncated and shifted fluid.

For a domain $\mathcal{B}$ that is bounded by $\partial\mathcal{B}$ the mass and momentum balances

$$\dot{\rho} + \rho\,\mathrm{div}\,\vec{v} = 0 \qquad\qquad \text{in} \qquad \mathcal{B} \qquad \text{, and} \tag{1}$$

$$\rho\dot{\vec{v}} = \mathrm{div}\,\boldsymbol{\sigma} + \rho\vec{g} \qquad \text{in} \qquad \mathcal{B} \qquad , \tag{2}$$

are solved for particle density $\rho(\vec{x}, t)$ and velocity $\vec{v}(\vec{x}, t)$. Position in space and time and gravitational acceleration are denoted by $\vec{x}$, t and $\vec{g}$. The material time derivative is denote by $\dot{(\cdot)} = \frac{\mathrm{d}(\cdot)}{\mathrm{d}t}$. The boundary conditions read

$$\vec{v} = \vec{0} \qquad \text{on} \qquad \partial\mathcal{B} \qquad , \tag{3}$$

$$\kappa\nabla\rho\cdot\vec{n} + \frac{\gamma_{\mathrm{sl}} - \gamma_{\mathrm{sv}}}{\rho' - \rho''}\left(30\varphi^4 - 60\varphi^3 + 30\varphi^2\right) = 0 \qquad \text{on} \qquad \partial\mathcal{B}\cap\partial\mathcal{B}_s \qquad \text{, and} \tag{4}$$

$$\nabla\rho\cdot\vec{n} = 0 \qquad \text{on} \qquad \partial\mathcal{B}\backslash\partial\mathcal{B}_s \qquad . \tag{5}$$

The outer normal to the boundary and the part of $\partial\mathcal{B}$ that is given by a solid surface are given by $\vec{n}$ and $\partial\mathcal{B}_s$. With $\varphi = \frac{\rho - \rho''}{\rho' - \rho''}$, where ρ' and ρ'' are the liquid and vapor bulk densities, (4) ensures a specified contact angle Θ for a droplet that is in contact with $\partial\mathcal{B}_s$, see also [4, 5]. The solid-liquid and solid-vapor surface tensions are denoted by γ_{sl} and γ_{sv}. The temperature T is assumed to be constant ($T = \mathrm{const.}$). The stress tensor $\boldsymbol{\sigma}$ reads

$$\boldsymbol{\sigma} = 2\eta\left[\nabla^{\mathrm{s}}\vec{v} - \frac{1}{3}\mathrm{tr}\left(\nabla^{\mathrm{s}}\vec{v}\right)\mathbf{1}\right] + \left(\rho a + \frac{\kappa}{2}|\nabla\rho|^2 - \rho\mu\right)\mathbf{1} - \kappa\nabla\rho\otimes\nabla\rho, \qquad \text{with} \qquad \mu = \frac{\partial\left(\rho a\right)}{\partial\rho} - \mathrm{div}(\kappa\nabla\rho), \tag{6}$$

and $\nabla^{\mathrm{s}}(\cdot) = \frac{1}{2}(\nabla(\cdot) + (\nabla(\cdot))^{\mathrm{T}})$, trace tr, dyadic product $\otimes$, and viscosity η. The free energy per particle $a = a(\rho, T)$ is taken from the PeTS equation of state [3] and the constant κ is set to $\kappa = 2.7334$ [1]. The Lennard-Jones dimensions are used for all physical quantities. They are nondimensionalized by using the convention $\sigma^{\mathrm{LJ}} = \varepsilon^{\mathrm{LJ}} = M^{\mathrm{LJ}} = 1$ for the size parameter, the energy parameter, and the mass per particle. Second derivatives in the weak form of the momentum balance (2) are avoided by using the chemical potential μ as an additional degree of freedom. For the finite element implementation, $\vec{v}$ is discretized with quadratic shape functions and ρ as well as μ with bi-linear shape functions (Q2P1). The backward Euler method is used for the time discretization.

---

* Corresponding author: e-mail fdiewald@rhrk.uni-kl.de, phone +49 (0) 631 205 3099, fax +49 (0) 631 205 2128

PAMM · Proc. Appl. Math. Mech. 2019;**19**:e201900091.   www.gamm-proceedings.com   **1 of 2**

https://doi.org/10.1002/pamm.201900091   © 2019 The Authors *Proceedings in Applied Mathematics & Mechanics* published by Wiley-VCH Verlag GmbH & Co. KGaA Weinheim
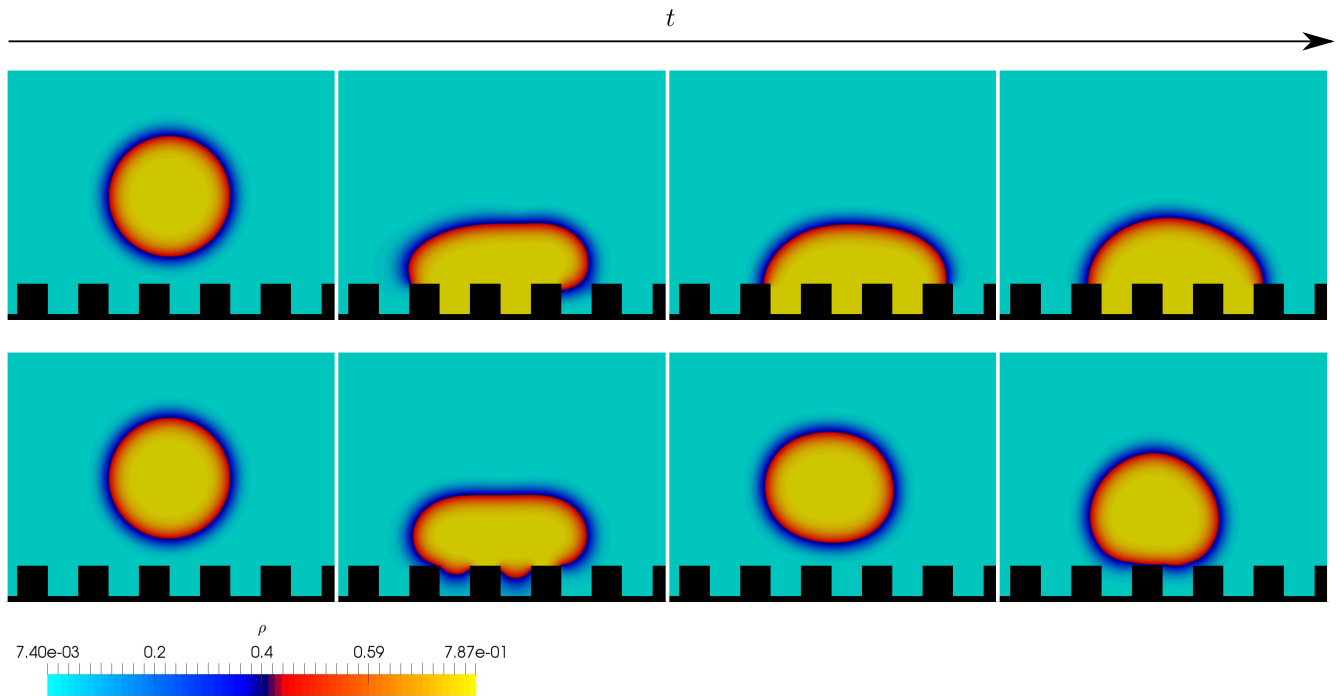
t

Fig. 1: Temporal evolution of droplet impact on structured component surface. Top: $\Theta = 90°$. Bottom: $\Theta = 150°$. The figures show snapshots of the density distribution for different times t. The droplet sinks into the structure for $\Theta = 90°$ and bounces off for $\Theta = 150°$.

2 Numerical Examples

In order to demonstrate the capability of the model to simulate dynamic wetting scenarios this section presents simulations of the impact of a droplet onto a structured component surface. A droplet is initialized with a radius of $r_{\text{ini}} = 5$ with its center $h_{\text{ini}} = 12.5$ above the bottom of the structured surface. The initial velocity in the entire computational domain is $\vec{v}_{\text{ini}} = \vec{0}$ and the gravitational acceleration is $\vec{g} = \begin{bmatrix} 0 & -0.01 \end{bmatrix}^{\text{T}}$. The temperature is set to $T = 0.7$, at which the surface tension between the liquid and the vapor phase is $\gamma_{\text{lv}} = 0.581$ [1]. The viscosity is $\eta = 0.01$. Two different combinations of γ_{sv} and γ_{sl} are considered. The first combination $\gamma_{\text{sv}} - \gamma_{\text{sl}} = 0.000$ leads to a theoretical contact angle of $\Theta = 90°$ (Young's equation $\Theta = \arccos(\frac{\gamma_{\text{sv}} - \gamma_{\text{sl}}}{\gamma_{\text{lv}}})$). The second combination $\gamma_{\text{sv}} - \gamma_{\text{sl}} = -0.503$ leads to a theoretical contact angle of $\Theta = 150°$. Snapshots of the temporal evolution of the droplet for the two combinations of of γ_{sv} and γ_{sl} are shown in Fig. 1. The top row of figures shows the simulation with a theoretical contact angle of $\Theta = 90°$ and the bottom row of figures the simulation with a theoretical contact angle of $\Theta = 150°$. The left most column of figures shows the droplet shortly before the impact. At this stage the results of the two simulations are identical. Once the droplet is in contact with the structured surface the temporal evolution of the two simulations differs. For $\Theta = 90°$ the droplet sinks into the structure and fills the grooves with liquid. For $\Theta = 150°$ the droplet does not sink into the structure. Instead, it bounces of and does not fill the grooves. A more detailed investigation of the second setup can help the development of self-cleaning surfaces. Future enhancements of the model will include a viscosity correlation that is based on molecular dynamics data.

References

[1] F. Diewald, M. Heier, M. Horsch, C. Kuhn, K. Langenbach, H. Hasse, and R. Müller, J. Chem. Phys. **149**, 064701 (2018).
[2] D. M. Anderson, G. B. McFadden, and A. A. Wheeler, Annu. Rev. Fluid Mech. **30**, 139-165 (1998).
[3] M. Heier, S. Stephan, J. Lui, W. G. Chapman, H. Hasse, and K. Langenbach, Mol. Phys. **116**, 2083-2094 (2018).
[4] M. Ben Said, M. Selzer, B. Nestler, D. Braun, C. Greiner, and H. Garcke, Langmuir **30**, 4033-4039 (2014).
[5] F. Diewald, C. Kuhn, M. Heier, K. Langenbach, M. Horsch, H. Hasse, and R. Müller, Comp. Mater. Sci. **141**, 185-192 (2018).